

EXTERNAL SHOCK IN A MULTI-BURSTING GAMMA-RAY BURST: ENERGY INJECTION PHASE INDUCED BY THE LATER LAUNCHED EJECTA

DA-BIN LIN^{1,2}, BAO-QUAN HUANG^{1,2}, TONG LIU³, WEI-MIN GU³, HUI-JUN MU³, AND EN-WEI LIANG^{1,2}

¹GXU-NAOC Center for Astrophysics and Space Sciences, Department of Physics, Guangxi University, Nanning 530004, China; lind-abin@gxu.edu.cn

²Guangxi Key Laboratory for the Relativistic Astrophysics, Nanning 530004, China

³Department of Astronomy, Xiamen University, Xiamen, Fujian 361005, China

ABSTRACT

Central engine of gamma-ray bursts (GRBs) may be intermittent and launch several episodes of ejecta separated by a long quiescent interval. In this scenario, an external shock is formed due to the propagation of the first launched ejecta into the circum-burst medium and the later launched ejecta may interact with the external shock at later period. Owing to the internal dissipation, the later launched ejecta may be observed at a later time (t_{jet}). In this paper, we study the relation of t_b and t_{jet} , where t_b is the collision time of the later launched ejecta with the formed external shock. It is found that the relation of t_b and t_{jet} depends on the bulk Lorentz factor (Γ_{jet}) of the later launched ejecta and the density (ρ) of the circum-burst medium. If the value of Γ_{jet} or ρ is low, the t_b would be significantly larger than t_{jet} . However, the $t_b \sim t_{\text{jet}}$ can be found if the value of Γ_{jet} or ρ is significantly large. Our results can explain the large lag of the optical emission relative to the γ -ray/X-ray emission in GRBs, e.g., GRB 111209A. For GRBs with a precursor, our results suggest that the energy injection into the external shock and thus more than one external-reverse shock may appear in the main prompt emission phase. According to our model, we estimate the Lorentz factor of the second launched ejecta in GRB 160625B.

Keywords: gamma-ray burst: general — ISM: jets and outflows — gamma-ray burst: individual (GRB 160625B)

1. INTRODUCTION

Observationally, gamma-ray bursts (GRBs) generally appear as a powerful burst of γ -rays followed by a long-lived afterglow emission. The light curves of afterglow emission usually can be decomposed into four power-law segments, i.e., an initial steep decay, a shallow decay, a normal decay, and a late steeper decay, together with one or several flares (Zhang et al. 2006; Nousek et al. 2006; O’Brien et al. 2006; Zhang et al. 2007). Theoretically, the phenomena of GRBs can be understood as follows. The central engine of a GRB, such as a stellar-mass black hole surrounded by a hyper-accretion disc (e.g., Narayan et al. 1992; Popham et al. 1999; Narayan et al. 2001; Gu et al. 2006; Liu et al. 2007) or a millisecond magnetar (Usov 1992; Thompson 1994; Dai & Lu 1998b; Wheeler et al. 2000; Zhang & Mészáros 2001; Metzger et al. 2008; Metzger et al. 2011; Bucciantini et al. 2012; Lü & Zhang 2014; Mösta et al. 2015), launches a relativistic ejecta, which may be composed of many mini-shells with different Lorentz factors. Then, the internal shocks (Rees & Meszaros 1994) or internal-collision-induced magnetic reconnection and turbulence (Zhang & Yan 2011; Deng et al. 2015) can be formed due to the collisions of shells. Owing to the powerful collisions, the prompt γ -rays are produced. The observed prompt γ -rays may also be released near the photosphere, where the ejecta becomes transparent for thermal photons. When the relativistic ejecta further propagates into the circum-burst medium, an external shock would be developed and thus produces a long-term broadband afterglow emission (Sari et al. 1998; Mészáros & Rees 1999; Sari & Piran 1999a,b). If there is no energy injection into the external shock, a normal decay would appear. However, the decay may become shallow during the continuous energy injection into the external shock (Zhang et al. 2006; Nousek et al. 2006; Panaitescu et al. 2006). This is the origin of the normal decay and shallow decay observed in the canonical light curve of afterglow emission. The initial steep decay phase in the afterglows is believed to be the tail emission of the prompt γ -rays (Barthelmy et al. 2005; Liang et al. 2006; O’Brien et al. 2006), and the late shallower decay is the external shock emission after the jet break phase.

The X-ray flares generally show sharp rise with a steep decay and thus may not be produced in the external shock. Similar to the formation of the prompt γ -rays, most of the X-ray flares are believed to be the internal origin (e.g., Romano et al. 2006; Falcone et al. 2006; Burrows et al. 2005; Falcone et al. 2006, 2007; Zhang et al. 2006; Nousek et al. 2006; Liang et al. 2006; Chincarini et al. 2007, 2010; Hou et al. 2014; Wu et al. 2013; Yi et al. 2015; Yi et al. 2016; Mu et al. 2016b; Mu et al. 2016a). It should be noted that the external-reverse shock (RS) is also adopted to explain the X-ray flares or prompt γ -rays in some burst (e.g., Shao & Dai 2005; Kobayashi et al. 2007; Fraija 2015; Fraija et al. 2016). Besides the X-ray flares, the X-ray plateau, e.g. GRBs 070110 and 060202 (Troja et al. 2007; Liang et al. 2007; Lü & Zhang 2014), or X-ray bump, e.g. GRBs 121027A and 111209A (Wu et al. 2013; Stratta et al. 2013; Yu et al. 2015), may also have the same physical origin as the prompt γ -rays. Thus, these X-ray plateau/bump are always dubbed “internal plateau/bump”. Most commonly, GRBs have a single episode of prompt γ -rays. However, some bursts show two or three episodes of prompt γ -rays separated by a long quiescent interval (~ 100 s), such as GRBs 110709B (Zhang et al. 2012) and 160625B (Zhang et al. 2016; Lü et al. 2017; Alexander et al. 2017; Fraija et al. 2017). In addition, 10% GRBs have a precursor emission, which may have the same physical origin as the prompt γ -rays (Troja et al. 2010; Hu et al. 2014). These observations suggested that the central engine of GRBs may be intermittent and launch several episodes of ejecta separated by a long quiescent interval. In this case, an external shock would be formed during the propagation of the first launched ejecta (JET1) into the circum-burst medium. The remnants of the later launched ejecta would catch up with the formed external shock at later period and thus the energy injection into the external shock would appear. The radiative signature associated with this process would appear through an external-forward shock (Sari et al. 1998; Sari & Piran 1999b) and/or an RS (Mészáros & Rees 1999; Sari & Piran 1999a,b). In this work, we focus on the observed time of the energy injection into the external shock.

The paper is organized as follows. In Section 2, we summarize the equations governing the evolution of the external shock. Here, the evolution of the external shock is estimated with energy injection from the remnants of the second launched ejecta (JET2). In Section 3, we estimate the observed time of the energy injection into the formed external shock. In Section 4, the conclusions and discussions are presented.

2. EVOLUTION OF THE EXTERNAL SHOCK WITH ENERGY INJECTION

We study the evolution of the external shock in the situation that the central engine of GRBs launches two episodes of ejecta separated by a long quiescent interval (t_{jet}). The external shock is formed during the propagation of JET1 into the circum-burst medium. Then, the remnants of JET2 would catch up with the formed external shock at the observer time t_b , and thus the energy injection into the external shock would appear at $t_{\text{obs}} \geq t_b$. In this section, we present the equations governing the evolution of the external shock.

Based on the conservation of energy and momentum, one can have (Piran 1999)

$$M' d\Gamma = -(\Gamma^2 - 1) dm \quad (1)$$

and

$$dU' = (1 - \varepsilon)(\Gamma - 1) dm c^2, \quad (2)$$

where Γ is the bulk Lorentz factor of the external shock, and $M' = M'_{\text{ej}} + m + U'/c^2$ is the total mass including the initial mass M'_{ej} of the ejecta, the sweep-up mass m from the circum-burst, and the internal energy U' of the external shock. Here, the physical quantities in the shell's/observer's frame are denoted with/without a prime. The radiated thermal energy in the shell's frame is described as $\varepsilon(\Gamma - 1) dm c^2$ with ε being the radiation efficiency of the external shock. The value of ε is assumed as a constant during the evolution of the external shock. Equation (1) can also be derived based on the relation between the total kinetic energy of the decelerated ejecta E_k and the radiated thermal energy (Huang et al. 1999), i.e.,

$$dE_k = -\varepsilon\Gamma(\Gamma - 1) dm c^2, \quad (3)$$

where $E_k = (\Gamma - 1)(M'_{\text{ej}} + m)c^2 + \Gamma U'$. With an energy injection dE_{inj} , Equation (3) can be modified as

$$dE_k = -\varepsilon\Gamma(\Gamma - 1) dm c^2 + dE_{\text{inj}}. \quad (4)$$

According to Equations (2) and (4), one can have

$$M' c^2 d\Gamma = dE_{\text{inj}} - (\Gamma^2 - 1) dm c^2 \quad (5)$$

or

$$\frac{d\Gamma}{dt_{\text{obs}}} = \frac{1}{M'} \left[\frac{1}{c^2} \frac{dE_{\text{inj}}}{dt_{\text{obs}}} - (\Gamma^2 - 1) \frac{dm}{dt_{\text{obs}}} \right], \quad (6)$$

which describes the evolution of Γ with respect to the observer time t_{obs} . The evolution of other parameters are described as

$$\frac{dU'}{dt_{\text{obs}}} = (1 - \varepsilon)(\Gamma - 1)c^2 \frac{dm}{dt_{\text{obs}}}, \quad (7)$$

$$\frac{dm}{dt_{\text{obs}}} = \frac{c\beta}{1 - \beta} 2\pi\rho R^2 (1 - \cos\theta_{\text{jet}}), \quad (8)$$

$$\frac{dR}{dt_{\text{obs}}} = \frac{c\beta}{1 - \beta}, \quad (9)$$

where $\beta = \sqrt{1 - 1/\Gamma^2}$ is the velocity of the external shock, ρ is the density of the circum-burst environment, and θ_{jet} is the half opening angle of the ejecta. The evolution of θ_{jet} is not considered in this work. Two cases of circum-burst medium, i.e., ISM and wind, are studied. Then, we take (e.g., [Chevalier & Li 2000](#))

$$\rho = \begin{cases} 5 \times 10^{11} A_* R^{-2} \text{ g} \cdot \text{cm}^{-1}, & \text{wind,} \\ n_0 m_p \text{ cm}^{-3}, & \text{ISM,} \end{cases} \quad (10)$$

with m_p being the proton mass.

Due to the internal dissipation of the ejecta, JET2 may be observed at the observer time t_{jet} . After this phase, the remnants of JET2 moves on and may collide with the formed external shock at later period. Then, the energy injection into the external shock may appear. To simplify our study, the function form of $dE_{\text{inj}}/dt_{\text{obs}}$ is described as

$$\frac{dE_{\text{inj}}}{dt} = \begin{cases} E_{\text{k,jet2}}/T_{\text{inj}}, & t_{\text{b}} < t_{\text{obs}} < t_{\text{b}} + T_{\text{inj}}, \\ 0, & \text{others,} \end{cases} \quad (11)$$

where $E_{\text{k,jet2}} = 10^{53}$ erg is taken as the remanent kinetic energy of JET2, $T_{\text{inj}} = \max(T_{90}, R_{\text{b}}/2\Gamma_{\text{jet2}}^2)$ is adopted, Γ_{jet2} ($T_{90} = 10$ s) is the Lorentz factor (duration of the prompt emission) of JET2, and the energy injection into the external shock is assumed to begin at the radius R_{b} and the observer time t_{b} . It should be noted that we are interested in the value of t_{b} rather than the details of energy injection.

To estimate the value of t_{b} , we trace the locations of JET2 and the external shock at every moment. If these two locations are the same, JET2 hits the external shock. The corresponding observer time is the value of t_{b} . Then, the energy injection as Equation (11) is added into the external shock. In our work, the evolution of the external shock is estimated with Equations (6)-(11) from the radius $R_0 = 10^{14}$ cm. In addition, the initial kinetic energy $E_{\text{k},0} = 10^{53}$ erg, the initial Lorentz factor $\Gamma_0 = 300$, $M'_{\text{ej}} = E_{\text{k},0}/(\Gamma_0 - 1)$, and the redshift $z = 1$ of the burst are adopted.

3. RESULTS

Figure 1 shows the evolution of the external shock in an ISM environment, where the JET2 with $(t_{\text{jet}}, \Gamma_{\text{jet2}}) = (30\text{s}, 300)$, $(100\text{s}, 300)$, $(30\text{s}, 100)$, and $(100\text{s}, 100)$ are adopted in the upper-left, upper-right, lower-left, and lower-right panels, respectively. In this figure, the red, black, and blue solid lines represent the X-ray (0.3-10 keV) flux from the external-forward shock in the situations with $n_0 = 10^{-2}$, 1, and 10^2 , respectively. The observed time (i.e., $[t_{\text{jet}}, t_{\text{jet}} + T_{90}]$) of JET2 emission is shown with a green horizontal line, and the values of t_{b} are indicated with a red, black, and blue vertical dashed lines for situations with $n_0 = 10^{-2}$, 1, and 10^2 , respectively. From Figure 1, it can be found that the observed time of the energy injection is larger than the observed time of JET2, i.e., $t_{\text{b}} > t_{\text{jet}}$. Moreover, the lower value of Γ_{jet2} or ρ is, the higher value of t_{b} would be. Then, we plot the relation of t_{b} and t_{jet} in Figure 2, where the value of $\Gamma_{\text{jet2}} = 300, 100$, and 30 are adopted in the upper, middle, and lower sub-figures, respectively. In this figure, ISM (wind) environment is adopted in the left (right) panels, the green dashed lines describe the relation of $t_{\text{b}} = t_{\text{jet}}$, and the blue, black, and red lines represent the situations with n_0 (or A_*) = 10^{-2} , 1, and 10^2 , respectively. According to Figure 2, the value of t_{b} can be significantly larger than that of t_{jet} . Lower value of Γ_{jet2} or ρ or t_{jet} is, the higher value of $t_{\text{b}}/t_{\text{jet}}$ would be. It is interesting to point out that $t_{\text{b}} \sim t_{\text{jet}}$ can be obtained if the value of Γ_{jet2} or ρ or t_{jet} is significantly large.

The dependence of t_{b} on Γ_{jet2} , ρ , and t_{jet} can be estimated as follows. After the internal dissipation, the JET2 is coasting forward. The observer time corresponding to the JET2 arriving at R can be estimated as

$$t_{\text{obs,jet2}}(R) = \frac{(R - R_{\text{dis}})(1 - \beta_{\text{jet2}})}{c\beta_{\text{jet2}}}(1 + z) + t_{\text{jet}}, \quad (12)$$

where $R_{\text{dis}} = 10^{14}$ cm (the dissipation location of JET2) and $\beta_{\text{jet2}} = \sqrt{1 - 1/\Gamma_{\text{jet2}}^2}$ are adopted in this paper. With Equations (1) and (2), the observed time of the external shock locating at R can be estimated as

$$t_{\text{obs}}(R) \approx \frac{R}{2\Gamma_0^2 c (1 + \beta m \Gamma_0 / M'_{\text{ej}})^\alpha} (1 + z), \quad (13)$$

where $\alpha = 2/(\varepsilon - 2)$, $\beta = -(2/\alpha)[- \alpha(3 - s) + 1]^{1/\alpha}$, and $\rho \propto R^{-s}$ are adopted. Then, the collision location R_{b} for JET2 catching up with the external shock can be found by taking $t_{\text{obs, jet2}} = t_{\text{obs}}$ or

$$\frac{(R_{\text{b}} - R_{\text{dis}})(1 - \beta_{\text{jet2}})}{c\beta_{\text{jet2}}} + \frac{t_{\text{jet}}}{1 + z} = \frac{R_{\text{b}}}{2\Gamma_0^2 c (1 + \beta m \Gamma_0 / M'_{\text{ej}})^\alpha}. \quad (14)$$

Accordingly, the observed time t_{b} of the collision can be estimated with

$$t_{\text{b}} = \frac{(R_{\text{b}} - R_{\text{dis}})(1 - \beta_{\text{jet2}})}{c\beta_{\text{jet2}}} (1 + z) + t_{\text{jet}}. \quad (15)$$

With Equations (14)-(15), we estimate the relation of t_{b} and t_{jet} for situations with $s = 0$ and $\Gamma_{\text{jet2}} = 100$. The results are shown with dashed lines in the middle-left panel of Figure 2, where the blue, black, and red dashed lines represent the situations with $n_0 = 10^{-2}$, 1, and 10^2 , respectively. It can be found that the value of t_{b} estimated based on Equations (14)-(15) is consistent with those estimated with Equations (6)-(9). According to Equation (14), one can find a low R_{b} and thus a low t_{b} in the situations with a larger Γ_{jet2} or ρ .

4. CONCLUSIONS AND DISCUSSIONS

Observations reveal that the central engine of GRBs may be intermittent and launch several episode of ejecta separated by a long quiescent interval. Owing to the internal dissipation, an episode of ejecta may be observed as a precursor, an episode of prompt γ -rays, an X-ray flare, an X-ray plateau, or an X-ray bump. In addition, an external shock is formed due to the propagation of the first launched ejecta into the circum-burst medium. Then, the later launched ejecta would collide with the formed external shock at a later time t_{b} . In this paper, we study the relation of t_{b} and t_{jet} , where t_{jet} is the observed time of the jet emission formed in the internal dissipation processes of the later launched ejecta. We find that the value of t_{b} can be significantly larger than that of t_{jet} . If the bulk Lorentz factor (Γ_{jet2}) of the later launched ejecta or the density (ρ) of the circum-burst medium is significantly low, the value of t_{b} may be significantly larger than t_{jet} . However, the situation of $t_{\text{b}} \sim t_{\text{jet}}$ can be found if the value of Γ_{jet2} or ρ or t_{jet} is significantly large. These results can explain the large lag of the optical emission relative to the γ -rays/X-rays observed in GRBs, e.g., the X-ray flare observed at $t_{\text{obs}} \sim 10^3$ s after the burst trigger in GRB 111209A.

Recently, an extremely bright GRB 160625B was detected by Fermi Gamma-Ray Burst Monitor and Large Area Telescope. Its prompt γ -ray lightcurve is composed of three episodes: a short precursor, a very bright main emission episode, and a weak later emission episode (Zhang et al. 2016). The three episodes emission are separated by two long quiescent intervals. Since the released energy in the first episode is lower than that in the second episode (Zhang et al. 2016), the value of t_{b} would be at around t_{jet} . Here, we assume that the bulk Lorentz factor of ejecta is proportional to the observed isotropic energy (e.g., Lü et al. 2014; Liang et al. 2015). That is to say, the remnants of the JET2 colliding with the external shock and the corresponding radiative signature would appear at around the observed time of the main prompt emission. An optical flash formed in this collision is indeed found in the main prompt emission phase (Lü et al. 2017). The situation is also applicable for GRB 140512A (Huang et al. 2016) and other bursts with a precursor. We note that the *Swift*/BAT is only triggered at the main prompt emission phase for some GRBs with a precursor (e.g., Hu et al. 2014). Then, we show the synthetic X-ray light curve from the burst trigger time for these GRBs. The results are shown in Figure 3, where the main prompt emission with isotropic energy $E_{\gamma, \text{iso}} = 10^{53}$ erg is shown with green solid lines, and $\Gamma_{\text{jet2}} = 500, 300,$ and 100 are adopted in the upper, middle, and lower panels, respectively. In this figure, the horizontal thick solid lines indicate the phase of the energy injection and the meanings of other lines are the same as those in Figure 1. In addition, the precursor is assumed to be observed at $t_{\text{obs}} = -30$ s (-100 s) in the left (right) panels of Figure 3. One can find that the light curve of X-rays does not behave as the form of a single bump. The energy injection into the external shock and thus an RS may appear in the phase of main prompt emission. Then, more than one RS may appear in or after the main prompt emission phase, e.g., GRB 130427A (Vestrand et al. 2014). One should be careful in dealing with the RS, especially for that in GRBs with a precursor. It is valuable to point out that the RS may also appear during the propagation of the JET1 into the circum-burst medium. In this situation, the evolution of the RS is discussed in two cases: thick- and thin-shell cases (e.g., Sari & Piran 1995;

Wu et al. 2003; Zou et al. 2005; Granot 2012; Yi et al. 2013; Fraija 2015). In the thick-shell case, the RS becomes relativistic during its propagation and the JET1 is significantly decelerated. The emission of the RS is overlapped with the emission of JET1. In the thin-shell case, the RS cannot decelerate the JET1 effectively and thus the emission of the RS may be lagged behind the emission of JET1. However, there is no energy injection (into the external shock) associated with the RS in this situation.

If the circum-burst environment and the energy injection time have been estimated, one can estimate the Lorentz factor of the ejecta producing X-ray flare/plateau/bump, and even those producing the main prompt emission for GRBs with a precursor. In Figure 4, we estimate the relations of t_b and $\Gamma_{\text{jet}2}$ for GRB 160625B in different situations, where t_b is the observed time of JET2 (i.e., the jet producing main prompt emission) colliding with the formed external shock and $z = 1.406$ (Xu et al. 2016) is adopted. In this figure, the situations with an ISM environment and $n_0 = 36$ (Lü et al. 2017) are shown with black lines, the situations with a wind environment and $A_* = 0.2$ (Fraija et al. 2017) are shown with red lines, and the situations with $E_{k,\text{iso}} = 8.8 \times 10^{52}$, 8.8×10^{51} , and 8.8×10^{50} erg are plotted with the dashed, solid, and dash-dotted lines, respectively. In GRB 160625B, an optical flash formed in the RS is found at the observer time 200 s (Lü et al. 2017). Then, we would like to believe that the energy injection into the formed external shock from JET2 appears at the observer time $t_b = 200$ s, which is shown with the blue dotted line in Figure 4. It can be found that the value of $\Gamma_{\text{jet}2} = 220$ (107) are required for the situations with $E_{k,\text{iso}} = 8.8 \times 10^{51}$ erg and ISM (wind) environment. It is worth noting another energetic burst GRB 130427A, which was observed in GeV-MeV γ -rays, X-rays, and the optical band. In order to explain the multiwavelength observations, Vestrand et al. (2014) claimed that more than one episode of energy injection and RS were necessary. In the time interval from 9.31 s to 19.31 s after the GBM trigger, a bright optical flash with a magnitude of 7.03 ± 0.03 is reported by RAPTOR (Vestrand et al. 2014). In addition, a bright LAT peak in coincidence with this optical flash is found (Ackermann et al. 2014). Then, Fraija et al. (2016) interpreted the bright optical flash/the extreme LAT peak as the synchrotron/synchrotron self-Compton emission from the RS when the deceleration of the ejecta evolves as that in the thick-shell case. For the other RS in this burst, the energy injection into the external shock is required (Vestrand et al. 2014). Since the jets being responsible for the energy injection are not observed definitely (see Figs. 1 and 2 in Ackermann et al. 2014), the relation of t_b and t_{jet} could not be estimated based on the observations of the other RS.

We thank Bing Zhang for helpful discussions. This work is supported by the National Basic Research Program of China (973 Program, grant No. 2014CB845800), the National Natural Science Foundation of China (grant Nos. 11773007, 11403005, 11533003, 11573023, 11473022), the Guangxi Science Foundation (grant Nos. 2016GXNSFDA380027), the Special Funding for Guangxi Distinguished Professors (Bagui Yingcai & Bagui Xuezhe), and the Innovation Team and Outstanding Scholar Program in Guangxi Colleges.

REFERENCES

- Ackermann, M., Ajello, M., Asano, K., et al. 2014, *Science*, 343, 42
- Alexander, K. D., Laskar, T., Berger, E., et al. 2017, arXiv:1705.08455
- Barthelmy, S. D., Cannizzo, J. K., Gehrels, N., et al. 2005, *ApJL*, 635, L133
- Bucciantini, N., Metzger, B. D., Thompson, T. A., & Quataert, E. 2012, *MNRAS*, 419, 1537
- Burrows, D. N., Romano, P., Falcone, A., et al. 2005, *Science*, 309, 1833
- Chevalier, R. A., & Li, Z.-Y. 2000, *ApJ*, 536, 195
- Chincarini, G., Moretti, A., Romano, P., et al. 2007, *ApJ*, 671, 1903
- Chincarini, G., Mao, J., Margutti, R., et al. 2010, *MNRAS*, 406, 2113
- Dai, Z. G., & Lu, T. 1998, *A&A*, 333, L87
- Deng, W., Li, H., Zhang, B., & Li, S. 2015, *ApJ*, 805, 163
- Falcone, A. D., Burrows, D. N., Lazzati, D., et al. 2006, *ApJ*, 641, 1010
- Falcone, A. D., Morris, D., Racusin, J., et al. 2007, *ApJ*, 671, 1921
- Fraija, N. 2015, *ApJ*, 804, 105
- Fraija, N., Lee, W. H., Veres, P., & Barniol Duran, R. 2016, *ApJ*, 831, 22
- Fraija, N., Lee, W., & Veres, P. 2016, *ApJ*, 818, 190
- Fraija, N., Veres, P., Zhang, B. B., et al. 2017, arXiv:1705.09311
- Granot, J. 2012, *MNRAS*, 421, 2442
- Gu, W.-M., Liu, T., & Lu, J.-F. 2006, *ApJL*, 643, L87
- Hou, S. J., Geng, J. J., Wang, K., et al. 2014, *ApJ*, 785, 113
- Hu, Y.-D., Liang, E.-W., Xi, S.-Q., et al. 2014, *ApJ*, 789, 145
- Huang, Y. F., Dai, Z. G., & Lu, T. 1999, *MNRAS*, 309, 513
- Huang, X.-L., Xin, L.-P., Yi, S.-X., et al. 2016, *ApJ*, 833, 100
- Kobayashi, S., Zhang, B., Mészáros, P., & Burrows, D. 2007, *ApJ*, 655, 391
- Liang, E. W., Zhang, B., O'Brien, P. T., et al. 2006, *ApJ*, 646, 351
- Liang, E.-W., Zhang, B.-B., & Zhang, B. 2007, *ApJ*, 670, 565
- Liang, E.-W., Lin, T.-T., Lü, J., et al. 2015, *ApJ*, 813, 116
- Liu, T., Gu, W.-M., Xue, L., & Lu, J.-F. 2007, *ApJ*, 661, 1025
- Lü, H.-J., & Zhang, B. 2014, *ApJ*, 785, 74
- Lü, H.-J., Lü, J., Zhong, S.-Q., et al. 2017, *ApJ*, 849, 71
- Lü, H.-J., Zhang, B., Liang, E.-W., Zhang, B.-B., & Sakamoto, T. 2014, *MNRAS*, 442, 1922
- Mészáros, P., & Rees, M. J. 1999, *MNRAS*, 306, L39

- Metzger, B. D., Quataert, E., & Thompson, T. A. 2008, *MNRAS*, 385, 1455
- Metzger, B. D., Giannios, D., Thompson, T. A., Bucciantini, N., & Quataert, E. 2011, *MNRAS*, 413, 2031
- Mösta, P., Ott, C. D., Radice, D., et al. 2015, *Nature*, 528, 376
- Mu, H.-J., Gu, W.-M., Hou, S.-J., et al. 2016, *ApJ*, 832, 161
- Mu, H.-J., Lin, D.-B., Xi, S.-Q., et al. 2016, *ApJ*, 831, 111
- Narayan, R., Paczynski, B., & Piran, T. 1992, *ApJL*, 395, L83
- Narayan, R., Piran, T., & Kumar, P. 2001, *ApJ*, 557, 949
- Nousek, J. A., Kouveliotou, C., Grupe, D., et al. 2006, *ApJ*, 642, 389
- O'Brien, P. T., Willingale, R., Osborne, J., et al. 2006, *ApJ*, 647, 1213
- Panaitescu, A., Mészáros, P., Gehrels, N., Burrows, D., & Nousek, J. 2006, *MNRAS*, 366, 1357
- Piran, T. 1999, *PhR*, 314, 575
- Popham, R., Woosley, S. E., & Fryer, C. 1999, *ApJ*, 518, 356
- Rees, M. J., & Mészáros, P. 1994, *ApJL*, 430, L93
- Romano, P., Moretti, A., Banat, P. L., et al. 2006, *A&A*, 450, 59
- Sari, R., & Piran, T. 1995, *ApJL*, 455, L143
- Sari, R., Piran, T., & Narayan, R. 1998, *ApJL*, 497, L17
- Sari, R., & Piran, T. 1999, *ApJL*, 517, L109
- Sari, R., & Piran, T. 1999, *ApJ*, 520, 641
- Shao, L., & Dai, Z. G. 2005, *ApJ*, 633, 1027
- Stratta, G., Gendre, B., Atteia, J. L., et al. 2013, *ApJ*, 779, 66
- Thompson, C. 1994, *MNRAS*, 270, 480
- Troja, E., Cusumano, G., O'Brien, P. T., et al. 2007, *ApJ*, 665, 599
- Troja, E., Rosswog, S., & Gehrels, N. 2010, *ApJ*, 723, 1711
- O'Brien, P. T., Willingale, R., Osborne, J., et al. 2006, *ApJ*, 647, 1213
- Usov, V. V. 1992, *Nature*, 357, 472
- Vestrand, W. T., Wren, J. A., Panaitescu, A., et al. 2014, *Science*, 343, 38
- Wheeler, J. C., Yi, I., Höflich, P., & Wang, L. 2000, *ApJ*, 537, 810
- Wu, X. F., Dai, Z. G., Huang, Y. F., & Lu, T. 2003, *MNRAS*, 342, 1131
- Wu, X.-F., Hou, S.-J., & Lei, W.-H. 2013, *ApJL*, 767, L36
- Xu, D., Malesani, D., et al. 2016, *GRB Coordinates Network*, 19600, 1
- Yi, S.-X., Wu, X.-F., & Dai, Z.-G. 2013, *ApJ*, 776, 120
- Yi, S.-X., Wu, X.-F., Wang, F.-Y., & Dai, Z.-G. 2015, *ApJ*, 807, 92
- Yi, S.-X., Xi, S.-Q., Yu, H., et al. 2016, *ApJS*, 224, 20
- Yu, Y. B., Wu, X. F., Huang, Y. F., et al. 2015, *MNRAS*, 446, 3642
- Zhang, B., Fan, Y. Z., Dyks, J., et al. 2006, *ApJ*, 642, 354
- Zhang, B.-B., Liang, E.-W., & Zhang, B. 2007, *ApJ*, 666, 1002
- Zhang, B., & Mészáros, P. 2001, *ApJL*, 552, L35
- Zhang, B., & Yan, H. 2011, *ApJ*, 726, 90
- Zhang, B.-B., Burrows, D. N., Zhang, B., et al. 2012, *ApJ*, 748, 132
- Zhang, B.-B., Zhang, B., Castro-Tirado, A. J., et al. 2016, *arXiv:1612.03089*
- Zou, Y. C., Wu, X. F., & Dai, Z. G. 2005, *MNRAS*, 363, 93

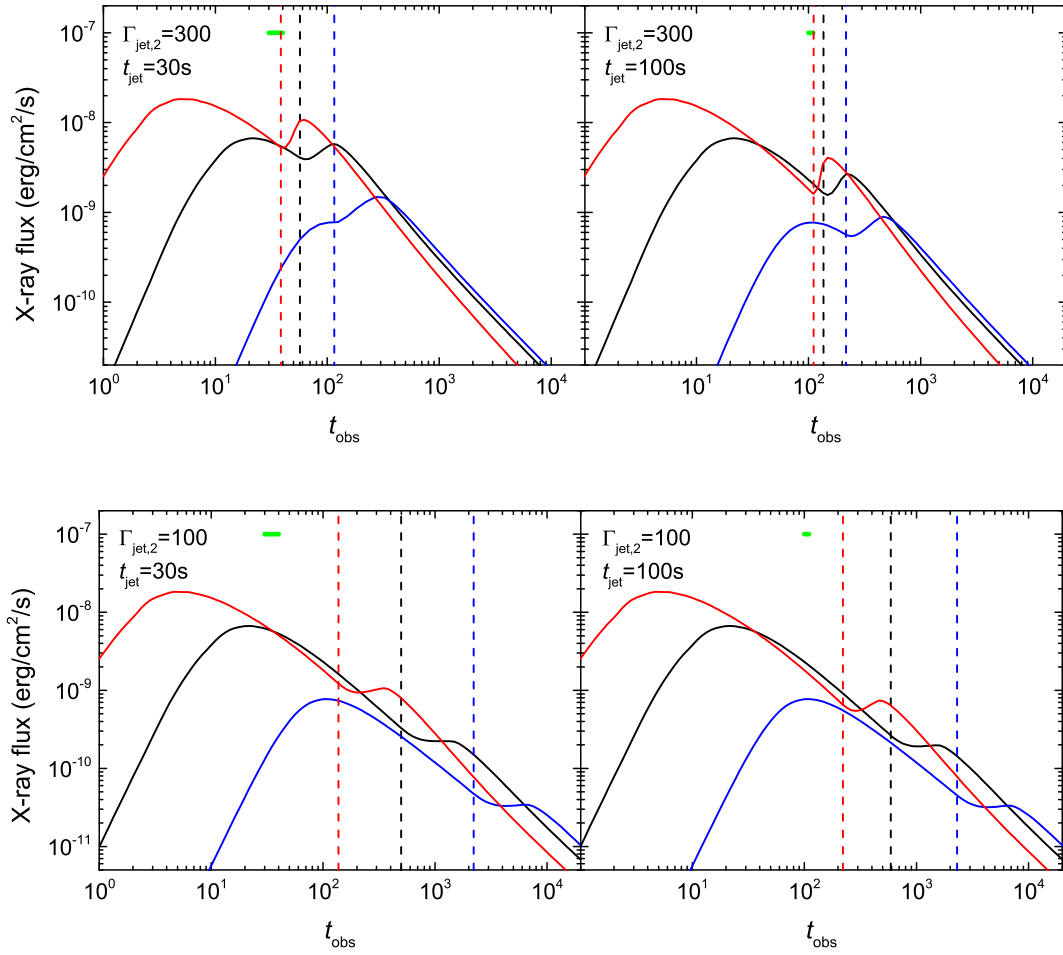


Figure 1. Evolution of the external shock with energy injection from the remnants of JET2, where $t_{\text{jet}} = 30$ s (100 s) is assumed in the left (right) panels and the value of $\Gamma_{\text{jet},2} = 300$ (100) is taken in the upper (lower) panels. The horizontal green thick lines show the observed time of the second launched ejecta, and the red, black, and blue solid lines (vertical dashed lines) represent the 0.3-10 keV X-ray flux (t_b) in the situation with $n_0 = 10^2$, 1, and 10^{-2} , respectively.

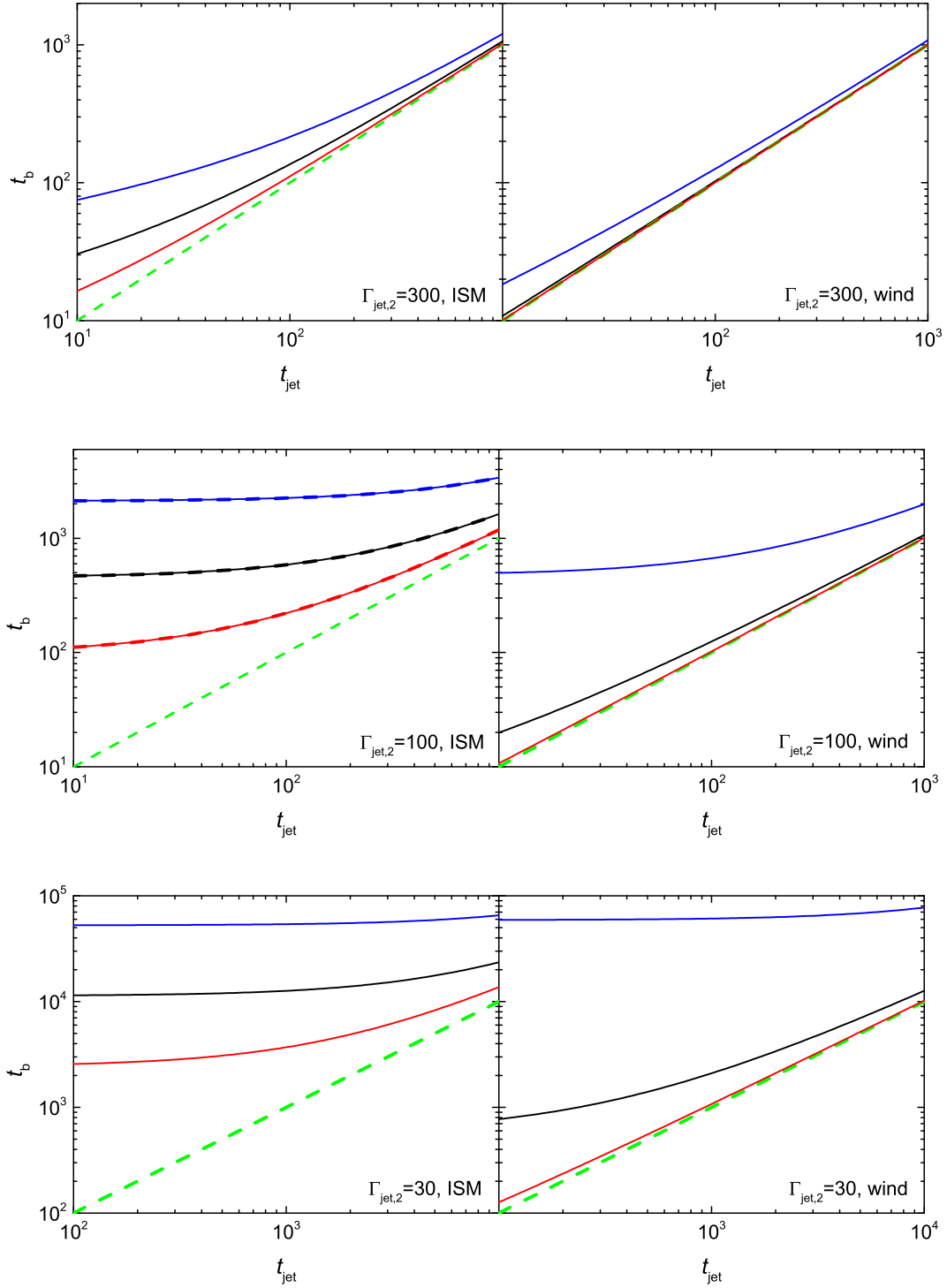


Figure 2. Comparison of t_b and t_{jet} . Here, the green dashed lines describe the relation of $t_b = t_{\text{jet}}$, the left (right) panels describe the situations with ISM (wind) environment, and $\Gamma_{\text{jet},2} = 300, 100,$ and 30 are adopted in the upper, middle, and lower sub-figures, respectively. The blue, black, and red solid lines in the left (right) panels represent the situations with $n_0(A_*) = 10^{-2}, 1,$ and $10^2,$ respectively.

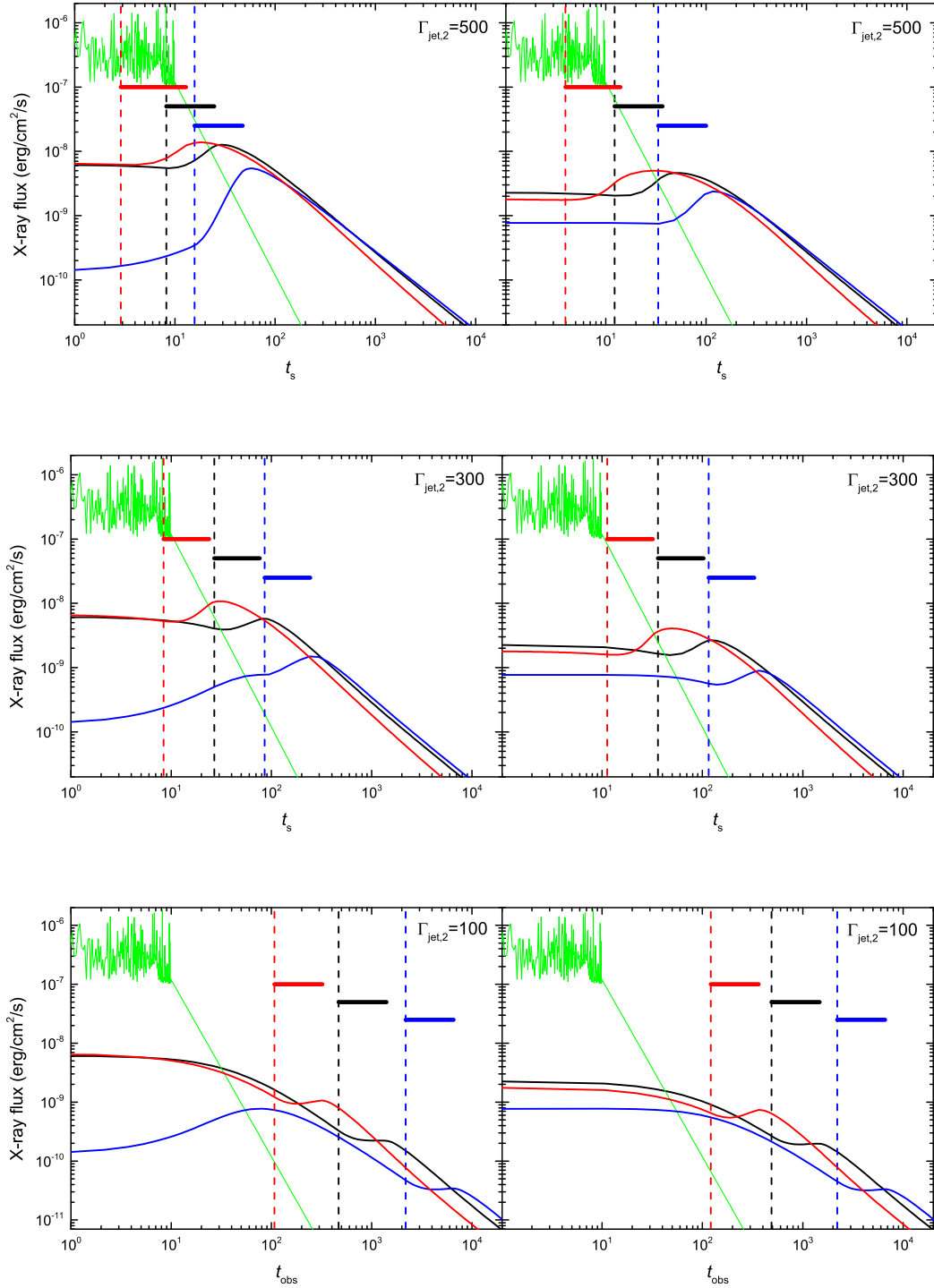


Figure 3. Synthetic X-ray light curve from the burst trigger time for GRBs with a precursor, where the main prompt emission (green solid lines) triggers the observation of BAT and the precursor is assumed to be observed at $t_{\text{obs}} = -30$ s (-100 s) in the left (right) panels. The thick red, black, and blue horizontal lines indicate the energy injection phase of the external shock and the meanings of other lines are the same as those in Figure 1.

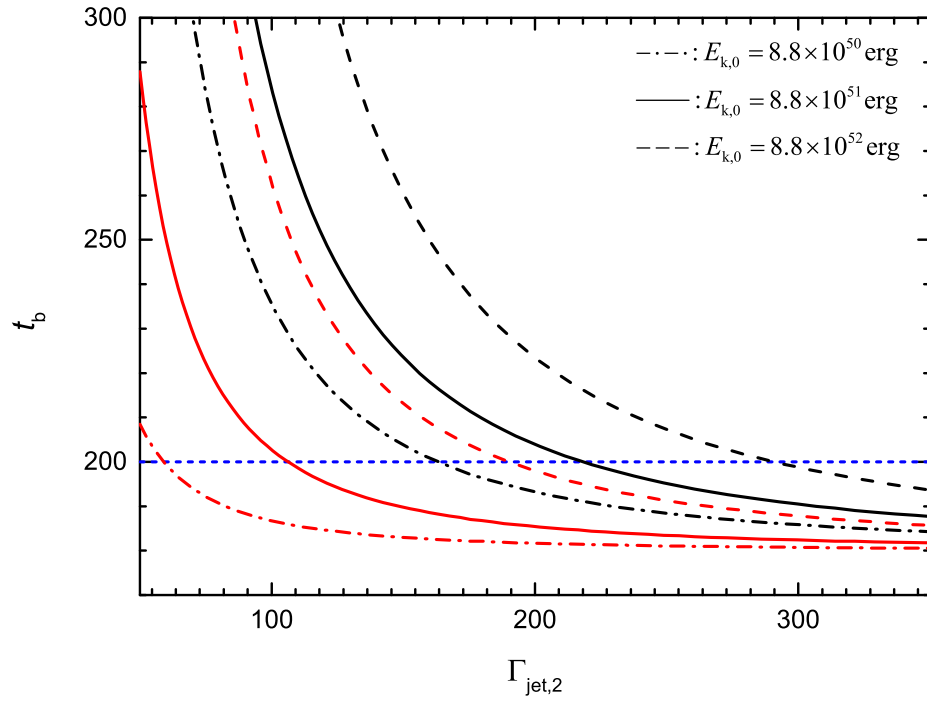


Figure 4. Relation of t_b and $\Gamma_{\text{jet},2}$ for GRB 160625B, where t_b is the observed time of JET2 hitting the external shock. The black lines are for the situations with an ISM environment and $n_0 = 36$, the red lines are for the situations with a wind environment and $A_* = 0.2$, and the dotted blue line indicates the observed time of the optical flash, i.e., $t_b = 200$ s.